Journal of the Neurological Sciences 372 (2017) 413–416

Contents lists available at ScienceDirect

Journal of the Neurological Sciences

journal homepage: www.elsevier.com/locate/jns

Microbleeds and cavernomas after radiotherapy for paediatric primary brain tumours

João Passos [a], Hipólito Nzwalo [b,*], Mariana Valente [a], Joana Marques [a], Ana Azevedo [a], Eduardo Netto [c], António Mota [c], Alexandra Borges [d], Sofia Nunes [e,f], Duarte Salgado [a,e]

[a] Neurology Department, Instituto Português de Oncologia de Lisboa Francisco Gentil, Portugal
[b] Biomedical Science and Medicine Department, Universidade do Algarve, Portugal
[c] Radiotherapy Department, Instituto Português de Oncologia de Lisboa Francisco Gentil, Portugal
[d] Radiology Department, Instituto Português de Oncologia de Lisboa Francisco Gentil, Portugal
[e] Paediatric Department, Instituto Português de Oncologia de Lisboa Francisco Gentil, Portugal
[f] Paediatric Neuro-Oncology Unit, Instituto Português de Oncologia de Lisboa Francisco Gentil, Portugal

ARTICLE INFO

Article history:
Received 14 July 2016
Received in revised form 30 October 2016
Accepted 3 November 2016
Available online 11 November 2016

Keywords:
Microbleeds
Cavernomas
Tumor
Focal hemosiderin deposition
Radiotherapy

ABSTRACT

Background: With the expected growth and aging of the population of primary central nervous system tumours (PCNST) survivors, attention to the radiation-induced late brain injury is fundamental. Late focal hemosiderin deposition (FHD) lesions, namely microbleeds and cavernomas, are among the presumable late cerebrovascular complications associated with radiotherapy for PCNST.
Objective: To explore association between PCNST radiotherapy and the occurrence FHD lesions and to address the correlation between the topographic location of these microvascular lesions with the focal radiotherapy location.
Methods: Retrospective cohort study of 190 paediatric patients being followed for PCNST in a single referral oncological centre. The frequency of FHD lesions was compared between paediatric PCNST treated ($n = 132$) and not treated ($n = 58$) with brain radiation. Microbleed Anatomical Rating Scale (MARS) was used for systematic identification of these cerebrovascular lesions and to address the consistency between the topographic location of each lesion and the location of the focal radiotherapy area. Univariate analysis to address the role of variables such as tumour histology, location, gender and age of children at the beginning of radiotherapy, duration of follow-up and chemotherapy was performed.
Results: FHD lesions (microbleeds and cavernomas) occurred exclusively and in a high percentage (41.6%) in PCNST survivors treated with brain radiation. Younger age at the diagnosis ($p = 0.031$), duration of follow-up ($p = 0.010$) and embryonal histology ($p = 0.003$) positively correlated with the occurrence FHD lesions. FHD lesions were topographically concordant with the brain focal irradiation area in 3/19 (15.8%) patients from the focal RT subgroup and in 22/111 (19.8%) patients from the WBRT plus focal RT subgroup.
Conclusion: Our study, which is one of the largest to date on the topic, shows that FHD lesions are a common complication after radiotherapy for childhood PCNST. The young brain is probably more susceptible to radiation-induced late cerebrovascular injury. Diffuse small vessel disease and ceiling effect may account for the low topographic concordance we found. The clinical implications of FHD lesions in this specific population are yet to be clarified.

1. Introduction

The overall survival of childhood primary central nervous system tumours (PCNST) increased in the last decades [1]. As this population ages, new challenges will rise to health care providers, with emphasis on the diagnosis and management of late sequelae from treatment, including radiation-induced cerebrovascular damage [2]. Microbleeds and cavernomas can be grouped as focal hemosiderin deposition (FHD) [3] and are imaging markers of radiation-induced small vessel disease (SVD) [4]. Both are best detected using either susceptibility-weighted imaging (SWI) or T2*-weighted gradient-recalled echo (GRE) sequences [3,5]. Microbleeds are also associated with cognitive impairment in the general population [5–7] and very recently, were found to be associated with neurocognitive dysfunction in PCNST survivors after radiotherapy (RT) [8]. The underling mechanism between RT and the occurrence of FHD is not yet fully understood. The purpose of

* Corresponding author at: Departement of Biomedical Sciences and Medicine, University of Algarve, Campus da Penha, 8005-139 Faro, Portugal.
E-mail address: nzwalo@gmail.com (H. Nzwalo).

http://dx.doi.org/10.1016/j.jns.2016.11.005
0022-510X/

the present study was to depict, quantify and locate FHD lesions, and to correlate its occurrence with the type, and topographic location of RT in childhood PCNST patients.

2. Methods

2.1. Study population

All paediatric patients with central nervous system tumours followed in our neuro-oncology unit from January 1973 to August 2015 were reviewed. Patients with at least 1 GRE sequence acquisition in our hospital's medical image database were included (this MRI sequence was introduced in our imaging protocol in 2006).

2.2. Data collection

All patients were regularly followed in a dedicated outpatient consultation, with at least one visit each year and at least one brain MRI each year. Data on demographic information (age, age at brain tumour diagnosis, gender, race), tumour characteristics (location, pathology), and treatment (resection, RT dose, RT volume, chemotherapy) were retrieved from the patients' electronic and manual clinical charts. Only the first GRE sequence acquisition was included in the present study.

2.3. Acquisition and imaging data extraction

Each MRI exam, including axial FSE T1 (TR/TE 543/12 ms, 280 × 168, 5/1 mm); FSE DP/T2; (TR/TE 3312/11/100 ms, 332 × 216, 5/1 mm); FLAIR (TR/TI/TE 11000/2800/140; 280 × 168, 5/1 mm); GRE T2* (TR/TE 760/23 ms; 280 × 168, 5/1 mm), 3D T1 after gadolinium (TR/TE 8.3/3.8 s, 256 × 256, 1/0 mm), was independently reviewed by a neuroradiologist (AB) and, at least, one neurologist (SN; AA; JP). Concordance rate was 78.2% (104/133). Discordant readings were reviewed, and consensus was achieved after discussion with the attending senior neuroradiologist (AB, with 15 years of experience). We used the Microbleed Anatomical Rating Scale (MARS) for topographic and quantitative characterization of FHD lesions [9]. RT volume was determined using 3D RT fields or inferred using pre-treatment images or clinical data validated by a radiation oncologist blinded for MARS' results. Microbleed was defined by the presence of a small rounded or ovoid well-defined hypointense lesion on GRE sequence, surrounded by brain parenchyma in at least half of the lesion (to avoid exclusion of cortical microbleeds), indistinct on T1 and T2-weighted MRI images (Fig. 1 – Illustrative images). A cut-off value of 2 mm was used and the potential mimickers (calcium deposits, vessel flow void and traumatic brain injury) were excluded by image or history [6]. All lesions within a 0.5 cm margin around the surgical resection site were excluded. We considered cavernoma all GRE lesions well seen on T1 or T2 that could be categorized using Zabramski cavernomas classification10: [Type I – hyperintense core on T1 and hypointense rim on T2 (subacute haemorrhage)]; [Type II – reticular core on both T1 and T2 and hypointense rim on T2 (loculated areas of haemorrhage and thrombosis of varying age, surrounded by gliotic, hemosiderin stained brain)]; [Type III – iso or hypointense on T1 and hypointense rim on T2 (chronic resolved haemorrhage)] (Fig. 1 – Illustrative images). Both microbleeds and cavernomas were grouped as FHD lesions for the present analysis. The RT treatment was categorized as either whole brain radiotherapy (WBRT), focal or a combination of the two (in the craniospinal treated patients, only brain RT was considered, so they all fell in the WBRT category).

2.4. Statistics

All variables were analysed using descriptive statistic measures. Proportions' comparison using chi-square tests and Student *t*-tests were used to evaluate the association between: FHD and RT; FHD and RT type; FHD location and RT field. Confidence intervals were calculated by exact methods and a significance level of 0.05 was considered. The analysis was performed using SPSS software for Windows. The retrospective chart review and the study were approved by the Institutional Review Board.

3. Results

Of the 579 paediatric patients with PCNST of our institutional database, 190 had at least one brain GRE imaging during the follow-up period. One-hundred and nine (57.3%) were male. The mean age at the diagnosis of PCNST was 8.2 years (range 0–16 years) and 7.5 years (range 0–15 years) for the RT treated ($n = 132$) and non-RT treated

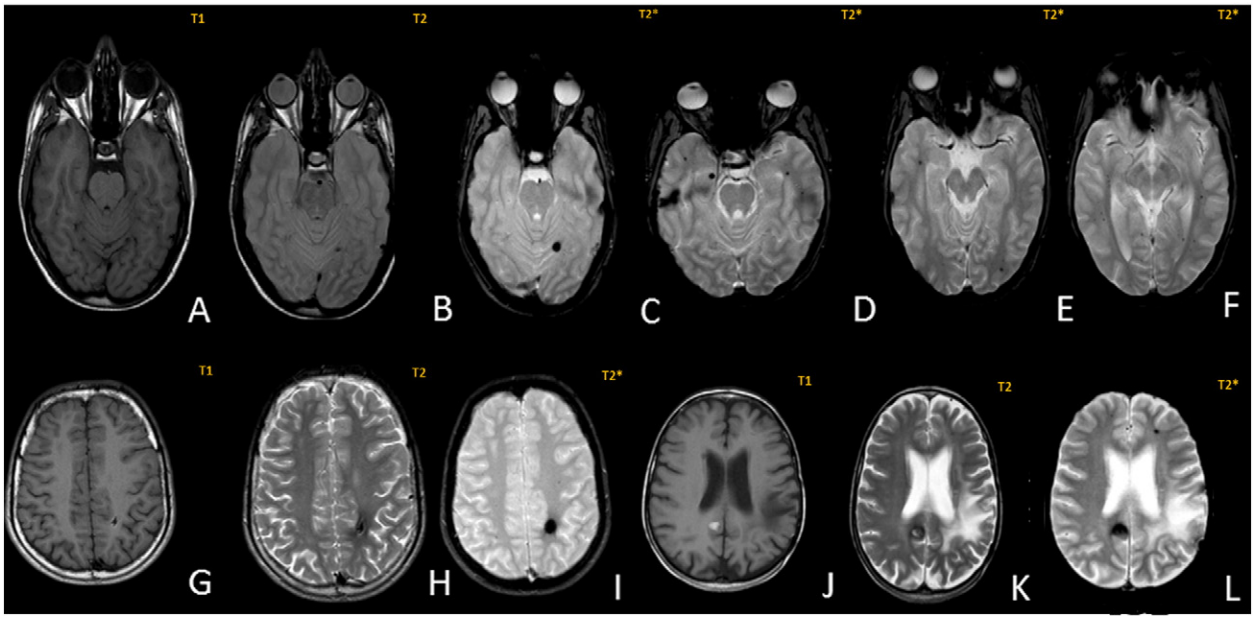

Fig. 1. Illustrative focal hemosiderin deposition lesions on axial brain magnetic resonance. Left occipital microbleed (A–C), coexistent multiple microbleeds (D–F), type 1 cavernoma on the left centrum semiovale (G–I), type III right parietal cavernoma and one microbleed on the right frontal lobe (J–L). T1 = T1 weighted image ; T2 = T1 weighted image; T2* = T2* weighted image.

group ($n = 58$) respectively. The median follow-up period was 133.0 months, with 15,005.0 patient-years of follow-up. Embryonal (42.4%), ependymal (17.4%) and low grade astrocytic (15.9%) tumours accounted for the majority of PCNST in the RT positive group, whereas low grade astrocytic (43.1%), embryonal (13.8%) and neuronal/mixed neuronal-glial (8.6%) tumours were the commonest PCNST in non-irradiated patients (Table 1). The differences in the clinical management between the RT positive and RT negative group expanded to other treatment modalities (chemotherapy, surgery or combination of both). The median and mean age at the end of RT was 8 and 8.3 years respectively. The majority of patients received a combination of WBRT plus focal RT (50.8%) or focal RT (46.2%). FHD lesions occurred in 55/41.6% patients, all in the RT positive group. A total of 133 FHD lesions were identified: 119 microbleeds and 14 cavernomas (3 type I, 1 type II and 10 type III). Topographic concordance analysis was performed in 53 patients (after exclusion of 2 WBRT patients with FHD lesions). The corresponding 129 lesions were distributed between two subgroups: focal RT, 12/61 (19.7%), with 19 lesions (mean 1.5, median 1.5 lesions/patient); WBRT plus focal RT, 41/67 (61.2%), with 111 FHD lesions (mean 2.6, median 2 lesions/patient). The FHD lesions were topographically concordant with the brain focal irradiation area in 3/19 (15.8%) patients from the focal RT subgroup and in 22/111 (19.8%) patients from the WBRT plus focal RT subgroup. Younger age at the time of diagnosis ($p = 0.031$), tumour histology ($p = 0.003$), longer follow-up ($p = 0.010$), WBRT treatment ($p < 0.001$), and longer time interval between RT treatment and GRE imaging ($p = 0.0007$) were associated with an increased risk of FHD lesions. Gender ($p = 0.588$) and age at RT ($p = 0.191$) were not associated with FHD lesions.

4. Discussion

In this large cohort of childhood PCNST, we have shown that FHD lesions, namely microbleeds and cavernomas, occurred exclusively in childhood PCNST patients treated with RT. In our analysis, we used the current international definitions for microbleeds and cavernomas [6,10] and grouped them under a broader designation (FHD), which covers a spectrum of imaging changes that are closely related [4]. FHD lesions occurred in a high percentage (41.6%) of PCNST patients treated with RT. We previously reported a smaller FHD prevalence (33%) among survivors of childhood PCNST treated with RT [4]. We believe that the systematic application of MARS improved the diagnostic sensitivity. Younger age at the diagnosis, embryonal histology, and the duration of follow-up were positively correlated with the diagnosis of microbleeds and cavernomas. Gender and age at RT treatment did not contribute to the occurrence of FHD. A thorough cavernoma characterization was beyond the scope of this study, nevertheless, the wide dispersion of lesion types (from I to III) suggests an ongoing dynamic brain SVD.

Both GRE acquisition with 5 mm slice thickness and the exclusion of smaller lesions (<2 mm) probably contributed for an underestimation of FHD, and we suspect that FHD prevalence may be higher. The topographic correlation between FHD and RT using MARS was low in both subgroups: 15.8% in focal RT and 19.8% in WBRT plus focal. More lesions per patient were found in the WBRT plus focal subgroup. We hypothesise that a ceiling effect accounts for the low topographic concordance between RT volume and FHD distribution in WBRT plus focal RT subgroup. Both subgroups were equally affected by the MARS

Table 1
Demographics, histology, treatment modalities and gradient echo signs changes in survivors of childhood PCNST.

Clinical variable		RT positive group ($n = 132$)		RT negative group ($n = 58$)	
		n	%	n	%
Gender	Female	51	38.6	30	51.7
	Male	81	61.4	28	48.3
Mean age at diagnosis (years)		8.2* (0–16)		7.5* (0–15)	
Histology	Embryonal	56	42.4	8	13.8
	Ependymal	23	17.4	4	6.9
	Low grade astrocytic	21	15.9	25	43.1
	Germ cell Tumour	19	14.4	3	5.2
	Neuronal/mixed neuronal-glial	1	0.8	5	8.6
	Without histologic diagnosis	1	0.8	4	6.9
	Other tumours	11	8.3	9	15.5
Treatment modalities	Sx alone	–	–	17	29,3
	CT alone	–	–	3	5,2
	CT + Sx	–	–	15	25,9
	No treatment	–	–	23	39,7
	CT + RT	8	6,1	–	–
	RT alone	3	2,3	–	–
	RT + Sx	36	27,3	–	–
	SX + RT + CT	85	64,4	–	–
Age of RT (years)		8.3 (1–17)		NA	NA
Radiotherapy modalities	WBRT + Focal	67	50.8	NA	NA
	Focal	61	46.2	NA	NA
	WBRT	4	3.0	NA	NA
RT doses (Gy)				NA	NA
Only WBRT ($n = 4$)[1]		38.0/40.0	24.0/50.0	NA	NA
WBRT combined with *boost* ($n = 67$)		34.7/36.0	17.2/40.0	NA	NA
Only focal ($n = 61$)[2]		53.2/54.0	24.0/60.0	NA	NA
Boost (focal combined with WBRT) $n = 67$		19.8/18.0	14.0/54.0	NA	NA
Medulla ($n = 57$)		34.1/36.0	23.0/40.0	NA	NA
Follow-up (years)		11.4/11.0* (0−32)		4.7/2.3* (0–32)	
GRE T2* lesions	MB	42	31.8%	–	–
	CV	2	1.5%	–	–
	MB + CV	11	8.3%	–	–
Time RT ↔ 1st T2* (years)		8.1 (0–24)		NA	NA
Time SX ↔ 1st T2* (years)		8.1 (0–24)		5.5 (0–32)	
Time CT ↔ 1st T2* (years)		8.1 (0–24)		5.3 (0–14)	
Age at 1st T2* (years)		16.9 (2–37)		11.6 (2–39)	

Sx: Surgery; CT: Chemotherapy; RT: Radiotherapy; WBRT:; MB:; CV: T2*: weighted gradient-recalled echo.

assessment limitations, since it does not account for the continuum of volume distribution that is key in focal RT characterization. RT fields' pathway may equally affect close anatomic structures that would be classified as non-related using MARS (cerebellum and occipital lobe, or temporal lobe and hypothalamus e.g.). In our opinion, the increased number of lesions in the WBRT subgroup is explained by the larger volume of brain parenchyma exposed to higher doses of radiation.

Ionizing radiation damage encompasses direct and indirect injury. [11] SVD after RT is most probably a dynamic process involving mechanisms such as increased expression of vascular endothelial growth factor (VEGF), blood brain barrier damage, oxidative stress and inflammation [11].

There is scarce literature addressing the clinical impact of FHD in this specific population. Cognitive dysfunction was very recently shown to be more common in survivors of paediatric brain tumour after cranial radiation therapy [8,12]. The risk of all type of strokes and of symptomatic intracerebral haemorrhage after thrombolysis for acute ischemic stroke is increased in the patients with microbleeds [13,14]. Direct extrapolations of this risk from the general population may not be appropriate. The underlying pathophysiology of deep brain or cortical microbleeds from hypertensive vasculopathy or amyloid vasculopathy respectively is very different from the radiation-induced SVD. In addition, patients with radiation-induced FHD are younger and have less comorbidities.

In conclusion, our study, which is one of the largest to date on the topic, showed that FHD lesions are common after RT for PCNST and occur diffusely in the brain. The high frequency of FHD lesions merits attention as a possible model for future preventive interventions. As PCNST survivors grow older, further investigation is warranted. Dose-volume characterization may clarify if there is any dose distribution dependence to these events and, in the future, help physicians tailor RT treatment. Longer follow-up studies will probably demonstrate the full scope of cerebrovascular damage in this population, and will certainly have an impact on the risk-benefit judgment prior to RT treatment.

Authors' contribution

Conception and design: João Passos; Sofia Nunes; Hipólito Nzwalo

Acquisition of data: Sofia Nunes; João Passos; Joana Marques; Mariana Valente; António Mota

Analysis and interpretation of MRI sequences: Alexandra Borges; Ana Azevedo; Sofia Nunes; João Passos

Statistical analysis: Sofia Nunes

Article drafting: João Passos; Hipólito Nzwalo; Sofia Nunes

Article review and final approval: all authors

Disclosure

The authors have nothing to disclose.

References

[1] L.A.G. Ries, M.A. Smith, J.G. Gurney, et al., Cancer Incidence and Survival among Children and Adolescents: United States SEER Program 1975–1995, National Cancer Institute, SEER Program. NIH Pub. No. 99–4649, Bethesda, MD, 1999.

[2] G.T. Armstrong, Q. Liu, Y. Yasui, et al., Long-term outcomes among adult survivors of childhood central nervous system malignancies in the Childhood Cancer Survivor Study, J. Natl. Cancer Inst. 101 (13) (Jul. 1 2009) 946–958.

[3] K.W. Yeom, R.M. Lober, et al., Increased focal hemosiderin deposition in pediatric medulloblastoma patients receiving radiotherapy at a later age, Nov 2013. J. Neurosurg. Pediatr. 12 (5) 444–451, http://dx.doi.org/10.3171/2013.7.PEDS1330 (Epub 2013 Aug 30).

[4] J. Passos, H. Nzwalo, J. Marques, et al., Late cerebrovascular complications after radiotherapy for childhood primary central nervous system tumors, Pediatr. Neurol. 53 (3) (Sep. 2015) 211–215.

[5] F. Fazekas, R. Kleinert, et al., Histopathologic analysis of foci of signal loss on gradient-echo T2*-weighted MR images in patients with spontaneous intracerebral hemorrhage: evidence of microangiopathy-related microbleeds, AJNR Am. J. Neuroradiol. 20 (4) (Apr. 1999) 637–642.

[6] A. Charidimou, A. Krishnan, D.J. Werring, et al., Cerebral microbleeds: a guide to detection and clinical relevance in different disease settings, Neuroradiology 55 (2013) 655–674.

[7] D.J. Werring, S.M. Gregoire, L. Cipolotti, Cerebral microbleeds and vascular cognitive impairment, Dec. 15 2010. J. Neurol. Sci. 299 (1–2) 131–135, http://dx.doi.org/10.1016/j.jns.2010.08.034 (Epub 2010 Sep 17).

[8] E. Roddy, K. Sear, et al., Presence of cerebral microbleeds is associated with worse executive function in pediatric brain tumor survivors, Neuro Oncol. (Aug. 18 2016) (pii: now163. Epub ahead of print).

[9] S.M. Gregoire, U.J. Chaudhary, M.M. Brown, et al., The microbleed anatomical rating scale (MARS): reliability of a tool to map brain microbleeds, Neurology 73 (21) (Nov. 24 2009) 1759–1766.

[10] J.M. Zabramski, T.M. Wascher, R.F. Spetzler, et al., The natural history of familial cavernous malformations: results of an ongoing study, J. Neurosurg. 80 (1994) 422–432.

[11] J.H. Kim, S.L. Brown, K.A. Jenrow, et al., Mechanisms of radiation-induced brain toxicity and implications for future clinical trials, J. Neurooncol 87 (3) (May 2008) 279–286.

[12] J.P. Warrington, N. Ashpole, A. Csiszar, et al., Whole brain radiation-induced vascular cognitive impairment: mechanisms and implications, 2013. J. Vasc. Res. 50 (6) 445–457, http://dx.doi.org/10.1159/000354227 (Epub 2013 Oct 1).

[13] A. Charidimou, A. Shoamanesh, D. Wilson, et al., Cerebral microbleeds and postthrombolysis intracerebral hemorrhage risk updated meta-analysis, Neurology 85 (11) (Sep. 15 2015) (927–4. in review).

[14] S. Akoudad, M.L. Portegies, P.J. Koudstaal, et al., Cerebral microbleeds are associated with an increased risk of stroke: the Rotterdam Study, Aug. 11 2015. Circulation 132 (6) 509–516, http://dx.doi.org/10.1161/CIRCULATIONAHA.115.016261 (Epub 2015 Jul 2).